Biochemistry

 Volume 33, Number 39 October 4, 1994

Articles

An Orally Bioavailable HIV-1 Protease Inhibitor Containing an Imidazole-Derived Peptide Bond Replacement: Crystallographic and Pharmacokinetic Analysis‡

Sherin S. Abdel-Meguid,*,§ Brian W. Metcalf,‖ Thomas J. Carr,‖ Peter Demarsh,⊥ Renee L. DesJarlais,# Seth Fisher,▽ David W. Green,▽,○ Lucinda Ivanoff,⊥ Dennis M. Lambert,⊥,+ Krishna H. M. Murthy,§,× Stephen R. Petteway, Jr.,⊥,+ William J. Pitts,‖,● Thaddeus A. Tomaszek, Jr.,‖ Evon Winborne,§ Baoguang Zhao,§ Geoffrey B. Dreyer,‖,☆ and Thomas D. Meek‖,○

Departments of Macromolecular Sciences, Medicinal Chemistry, Molecular Virology and Host Defense, Physical and Structural Chemistry, and Protein Biochemistry, SmithKline Beecham Pharmaceuticals, 709 Swedeland Road, King of Prussia, Pennsylvania 19406

Received May 26, 1994®

ABSTRACT: (2*R*,4*S*,5*S*,1′*S*)-2-Phenylmethyl-4-hydroxy-5-(*tert*-butoxycarbonyl)amino-6-phenylhexanoyl-*N*-(1′-imidazo-2-yl)-2′-methylpropanamide (compound **2**) is a tripeptide analogue inhibitor of HIV-1 protease in which a C-terminal imidazole substituent constitutes an isoelectronic, structural mimic of a carboxamide group. Compound **2** is a potent inhibitor of the protease (K_i = 18 nM) and inhibits HIV-1 acute infectivity of CD4+ T-lymphocytes (IC_{50} = 570 nM). Crystallographic analysis of an HIV-1 protease–compound **2** complex demonstrates that the nitrogen atoms of the imidazole ring assume the same hydrogen-bonding interactions with the protease as amide linkages in other peptide analogue inhibitors. The sole substitution of the C-terminal carboxamide of a hydroxyethylene-containing tripeptide analogue with an imidazole group imparts greatly improved pharmacokinetic and oral bioavailability properties on the compound compared to its carboxamide-containing homologue (compound **1**). While the oral bioavailability of compound **1** in rats was negligible, compound **2** displayed oral bioavailabilities of 30% and 14%, respectively, in rats and monkeys.

An essential, late step in the life cycle of human immunodeficiency virus (HIV) and other retroviruses is the proteolytic maturation of two polyprotein precursors catalyzed by a virally-encoded protease (Debouck et al., 1987; Meek et al., 1990a,b). The HIV-1 protease is an aspartic protease but differs from other enzymes of this class such as pepsin and renin, which are monomers, in that its structure is achieved by the assembly of two 11-kDa polypeptides into a functional homodimer (Meek et al., 1989; Wlodawer et al., 1989). Since the initial characterization of this enzyme, rapid progress has been made toward the development of highly potent peptide analogue inhibitors, predicated in large part on the structures of transition-state analogues proven to be effective for the monomeric aspartic proteases (Meek, 1992). From the

‡ The refined coordinates for the protease-inhibitor complex have been deposited in the Protein Data Bank under file name 1SBG.

* Author to whom correspondence should be addressed.
§ Department of Macromolecular Sciences.
‖ Department of Medicinal Chemistry.
⊥ Department of Molecular Virology and Host Defense.
Department of Physical and Structural Chemistry.
▽ Department of Protein Biochemistry.
○ Present address: Bristol-Myers Squibb Pharmaceutical Research Institute, Princeton, NJ 08543-4000.
+ Present address: Trimeris Inc., Two University Place, Durham, NC 27707.
× Present address: Fels Institute for Cancer Research and Molecular Biology, 3307 N. Broad St., Philadelphia, PA 19140.
● Present address: Dupont Merk Pharmaceutical Company, Experimental Station, E 353/341, Wilmington, DE 19880.
☆ Present address: Onyx Pharmaceuticals, 3031 Research Dr., Richmond, CA 94806.

® Abstract published in *Advance ACS Abstracts*, September 1, 1994.

0006-2960/94/0433-11671$04.50/0

Scheme 1

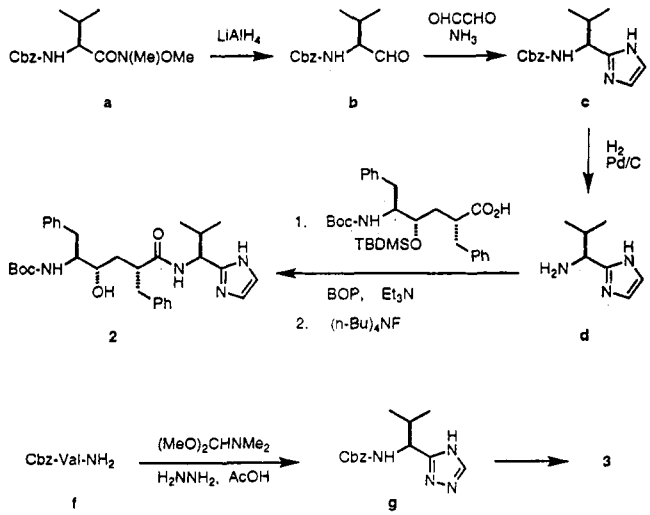

numerous crystal structures of HIV-1 protease-inhibitor complexes (Wlodawer & Erickson, 1993), it is now well established that the binding of these compounds involves the formation of a highly conserved series of hydrogen bonds between amide groups on the peptide analogues and complementary groups on the enzyme. In addition, the secondary alcohol within hydroxyethylene isostere-containing inhibitors forms hydrogen bonds with the active site aspartyl residues Asp25 and Asp25′ (Dreyer et al., 1992).

However, the pharmacokinetic and bioavailability properties of peptide analogue inhibitors of the aspartic proteases remain an impediment to the development of these compounds as drugs (Greenlee, 1990). It is thought that high lipophilicity, molecular weights greater than 500, and the presence of numerous amide bonds in these compounds are contributory to less desirable pharmacokinetic properties, as well as metabolic instability. Accordingly, the development of improved HIV-1 protease inhibitors into drug development candidates will require novel chemical strategies to address these issues, in particular, the replacement of amide bonds by peptidomimetic surrogates. In this report we describe the mimicry, in a tripeptide analogue inhibitor, of an amide bond by an imidazole substituent, resulting in a substantial improvement of its pharmacokinetic properties and its oral bioavailability.

EXPERIMENTAL PROCEDURES

Synthesis of Inhibitors

Tetrahydrofuran (THF)[1] was distilled from a sodium benzophenone ketyl. Ether refers to commercial anhydrous ethyl ether. All other reagents were from commercial sources and used without further purification. Flash chromatography was performed with E. Merck Kieselgel 60. Proton nuclear magnetic resonance (^{1}H NMR) spectra were recorded at 400 MHz on a Bruker AC 400 spectrometer. The synthesis of compound **1** has been previously described (Dreyer et al., 1992). The synthesis of compounds **2** and **3** are outlined in Scheme 1.

(Benzyloxycarbonyl)valinal (b). Amide **a** (5.3 g) [prepared by the procedure of Goel et al. (1989)] was added to a fine suspension of $LiAlH_4$ (0.821 g) in ether (80 mL) at −45 °C under Ar while stirring. After 5 min, the mixture was allowed to warm to 10 °C over 30 min and was then recooled to −45 °C, after which a solution of 7.0 g of $KHSO_4$ in 20 mL of water was added slowly. The cooling bath was removed, and the mixture was stirred for 30 min. Ether (100 mL) and CH_2Cl_2 (100 mL) were added, the mixture was filtered through Celite, and the filter cake was rinsed with 100 mL of ether. The filtrate was extracted with ice-cold 1 N HCl (3 × 50 mL), ice-cold 5% Na_2CO_3 (3 × 50 mL), and 100 mL of brine and then was dried over $MgSO_4$, filtered, and concentrated by rotary evaporation at 30 °C to provide **b** (3.74 g, 88% yield) as a white solid.

(1′S)-1′-Carbobenzyloxyamino-1′-isopropyl-1′-(imidazo-2-yl)methane (c). Aldehyde **b** (4.6 g) and glyoxal trimer dihydrate (1.33 g) were stirred in 100 mL of MeOH at −10 °C. Ammonia was bubbled through the solution for several minutes, and the mixture was allowed to stir at −10° C for 4 h. The mixture was then allowed to warm to room temperature over 14 h and then was poured into 250 mL of water. The suspension was filtered, and the filter cake was washed twice with water to give **c** (1.9 g, 36% yield) as a white solid. ^{1}H NMR (CD_3OD): δ 7.28 (5H, m), 6.89 (2H, s), 5.04 (2H, dd), 4.46 (1H, d), 2.10 (1H, m), 0.91 (3H, d), 0.70 (3H, d).

(1S)-1-Amino-1-isopropyl-1-(imidazo-2-yl)methane (d). Imidazole **c** (1.9 g) was stirred in 75 mL of MeOH over 10% Pd/C (200 mg). Hydrogen was bubbled through the solution for 1 h, and the solution was maintained under a hydrogen atmosphere overnight. The mixture was filtered through Celite and was evaporated to give **d** (720 mg, 75% yield) as a tacky solid.

(2R,4S,5S,1′S)-2-Phenylmethyl-4-hydroxy-5-(tert-butoxycarbonyl)amino-6-phenyl-N-[1′-isopropyl-1′-(imidazo-2-yl)]methylhexanamide hydrochloride (2). Imidazole **d** (48 mg), BOP reagent (168 mg), and triethylamine (0.053 mL) were added to a solution of (*2R,4S,5S*)-2-phenylmethyl-4-(*t*-butyldimethyl)siloxy-5-(*tert*-butoxycarbonyl)amino-6-phenylhexanoic acid (Dreyer et al., 1992) (200 mg) in CH_2Cl_2. The mixture was stirred overnight under argon and washed successively with water, 5% aqueous $NaHCO_3$, and saturated aqueous NaCl. The solution was dried over $MgSO_4$, filtered, and evaporated to give a white solid that was chromatographed (silica, 4% MeOH/CH_2Cl_2) to give TBDMS-protected **2** (**e**) as a white solid. Compound **e** (140 mg) was stirred in THF at room temperature under Ar. Tetrabutyl ammonium fluoride (0.38 mL) was added, and the solution was stirred overnight. The mixture was diluted with water and extracted with CH_2Cl_2 (3 × 50 mL). The combined organic extracts were washed with water and evaporated. The residue was treated with 1 equiv of methanolic HCl, concentrated, and triturated with ether and ethyl acetate to give **2** (95 mg, 83% yield) as a white solid. ^{1}H NMR (DMSO-D_6): δ 7.78 (1H, d), 7.16 (10H, m), 6.71 (2H, s), 6.39 (1H, d), 4.68 (1H, m), 4.52 (1H, d), 2.71 (3H, m), 2.48 (3H, m), 1.97 (1H, m), 1.61 (1H, m), 1.30 (9H, s), 0.78 (3H, d), 0.61 (3H, d). MS (DCl/NH_3): *m/z* 535.4 $(M + H)^+$. Analysis, calculated/found: C, 69.64/69.66; H, 7.92/7.97; N, 10.48/10.52.

(Benzyloxycarbonyl)valinamide (f). *N*-Methylmorpholine (11 mL) was added to a solution of carbobenzyloxy-L-valine (25 g) in 200 mL THF at −40 °C, and the mixture was stirred for 5 min. Isobutyl chloroformate (13 mL) was added; 5 min later 10 mL of liquid ammonia was introduced. After 30 min of vigorous stirring, the mixture was filtered, and the filter cake was washed with water, followed by ether. The solid

[1] Abbreviations: BOP, benzotriazol-1-yloxy-tris(dimethylamino)phosphonium hexafluorophosphate; DTT, dithiothreitol; EDTA, ethylenediaminetetraacetic acid; MES, 2-(*N*-morpholino)ethanesulfonic acid; rms, root mean square; TBDMS, *tert*-butyldimethylsilyl; t-Bu, *tert*-butyl; THF, tetrahydrofuran.

was dried to give **f** (20 g, 80% yield) as a white solid.

(1S)-1-Carbobenzyloxyamino-1-isopropyl-1-(1,2,4-triazo-3-yl)methane (g). Amide **f** (1.25 g) and *N,N*-dimethylformamide dimethylacetal (0.73 mL) were stirred in 4 mL of dimethylformamide at room temperature for 4 h. Acetic acid (4 mL) was added, and the mixture was stirred for 30 min. Hydrazine (0.16 mL) was added dropwise, and the mixture was heated at 90 °C for 2 h. The mixture was poured into 100 mL of Na_2CO_3 and then filtered. The solid was recrystallized from MeOH-water to give **g** (1.2 g, 88% yield) as a white solid. ^{1}H NMR ($CDCl_3$): δ 8.07 (1H, s), 7.45–7.20 (5H, m), 6.02 (1H, brd; J = 4 Hz), 5.12 (2H, t; J = 6 Hz), 4.82 (1H, t; J = 4 Hz), 2.25 (1H, m), 0.90 (6H, dd; J = 14, 6 Hz).

(2R,4S,5S,1'S)-2-Phenylmethyl-4-hydroxy-5-(tert-butoxycarbonyl)amino-6-phenylhexanoyl-N-1'-(1,2,4-triazo-3-yl)-2'-methylpropanamide (3). Compound **3** was prepared from amine **g** and (*2R,4S,5S*)-2-phenylmethyl-4-(*tert*-butyldimethyl)siloxy-5-(*tert*-butoxycarbonyl)amino-6-phenylhexanoic acid as described for compound **2**. ^{1}H NMR (CD_3OD): δ 0.65 (3H, d; J = 3 Hz), 0.85 (3H, d; J = 3 Hz), 1.30 (9H, s), 1.55 (1H, t; J = 3 Hz), 1.62 (1H, t; J = 3 Hz), 1.97 (1H, m), 2.50–2.83 (5H, m), 3.49 (1H, d; J = 4 Hz), 3.62 (1H, t; J = 1 Hz), 4.72 (1H, d; J = 3 Hz), 6.20 (1H, d; J = 4 Hz), 6.90–7.40 (10H, m), 8.12 (1H, s(br)). MS (ES/MS +/–): m/z 536.2 $(M + H)^+$.

Assays

Recombinant HIV-1 protease (Debouck et al., 1987) was prepared and purified to apparent homogeneity as previously described (Grant et al., 1991). Recombinant simian immunodeficiency virus (SIV) protease was prepared by the procedure of Grant et al. (1991), while HIV-2 protease was purchased from Bachem Bioscience Inc. (Philadelphia, PA). Porcine pepsin and bovine spleen cathepsin D were obtained from Boehringer Mannheim, and human renin was obtained from United States Biochemical Corporation. These enzymes were assayed as previously described (Dreyer et al., 1993; Meek et al., 1990b). For the retroviral proteases, inhibition constants (K_i) were determined for synthetic inhibitors as previously described (Dreyer et al., 1992) in a buffer containing 50 mM MES, pH 6.0, 1 mM EDTA, 1 mM DTT, 0.2 M NaCl, 0.1% Triton X-100, and 10% dimethyl sulfoxide at 37 °C.

The effects of the synthetic inhibitors on the acute infectivity of either H9 or Molt 4 cells by HIV-1 [HTLV-III$_B$ isolate (Ratner et al., 1985)] has been previously described (Lambert et al., 1992). Serial dilutions of protease inhibitors were obtained from stock solutions in 100% dimethyl sulfoxide and added to cell cultures at the time of infection. The starting concentrations of inhibitors were maintained for 7 days at which time HIV-1 infectivity was assessed by assay of reverse transcriptase activity.

Crystallography

The complex of compound **2** with HIV-1 protease was crystallized as described previously (Miller et al., 1989). Briefly, cocrystals were grown by the method of vapor diffusion in hanging drops (McPherson, 1976) by using 18–26% saturated ammonium sulfate buffered at pH 5.0 with 200 mM acetate as the precipitant. The symmetry of the diffraction was consistent with that of the hexagonal space group $P6_122$ or $P6_1$, with strong noncrystallographic 22 symmetry reflecting the 2-fold symmetry of the protein. We chose the latter space group to be consistent with the previously reported crystal structures of HIV-1 protease-inhibitor complexes (Erickson et al., 1990; Abdel-Meguid et al., 1993; Dreyer et al., 1992, 1993). The unit cell dimensions were $a = b = 63.4$ Å and $c = 83.7$ Å, with the asymmetric unit containing one complete copy of the complex (a protein dimer plus an inhibitor).

X-ray diffraction data were measured from a single crystal using a Siemens two-dimensional position-sensitive detector. The detector was mounted on a Siemens rotating anode X-ray generator operated at 50 kV and 96 mA, equipped with a 300-μm focusing cup, and producing graphite-monochromated Cu Kα radiation. Diffraction images were recorded, reduced, and visualized using FRAMBO, XENGEN (Howard et al., 1987) and XPREP computer programs, respectively. Approximately 36 380 reflections were measured in 2 days to give 8108 unique reflections to 2.3-Å resolution, representing 95% of the data. The merging R factor for symmetry-related reflections (R_{sym}) was 0.052 ($R_{sym} = \sum\sum|I_{i(h)} - \bar{I}_{(h)}|/\sum I_{i(h)}$, where $I_{i(h)}$ are the intensities of multiple measurements of reflection h and $\bar{I}_{(h)}$ is their mean).

Crystallographic refinement was carried out using the restrained least-squares program PROLSQ (Hendrickson, 1985). Minor modifications to the export version (Smith et al., 1988) of this program allowed for its use on a Silicon Graphics IRIS 4D/380 computer and for the ability to run multiple cycles of refinement without manual intervention. The starting model used in the refinement consisted of the protein portion of the 2.8-Å structure of A74704 complexed to HIV-1 protease (Erickson et al., 1990). A few cycles of rigid body least-squares refinement using data to 3.0-Å resolution for reflections greater than $3\sigma(F_o)$ were carried out to obtain the optimal position and orientation of the starting model. This was followed by iterative cycles of refinement and model building. Fourier maps with coefficients $|F_o| - |F_c|$ and $2|F_o| - |F_c|$ were computed and displayed on an Evans and Sutherland PS300 graphics system using FRODO (Jones, 1985). Maps calculated using refined phases, obtained from data greater than $2.0\sigma(F_o)$ in the resolution range of 8.0–2.5 Å, showed electron density for the inhibitor.

A model of compound **2** was positioned in the electron density, and the complex was further refined; special bond and angle distances were incorporated in the program PROTIN (Hendrickson, 1985) to account for the geometry of the inhibitor. This was followed by refinement using XPLOR (Brunger et al., 1987) for comparison. Results from both PROLSQ and XPLOR refinement were very similar. Refinement resulted in a final crystallographic R factor of 0.188 ($R = \sum|F_o| - |F_c|/\sum|F_o|$, where F_o and F_c are the observed and calculated structure factor amplitudes, respectively) for the data between 6.0- and 2.3-Å resolution. The overall rms deviation from ideal geometry for bond lengths was 0.018 Å, while that for bond angles was 3.83°. The refined set of atomic coordinates has been deposited in the Protein Data Bank (PDB; Bernstein et al., 1977).

Evaluation of Pharmacokinetics and Bioavailability of Protease Inhibitors in Rats and Monkeys

Dual-jugular cannulated Sprague Dawley rats (200–250 g) were treated either intravenously with a dosing solution (1–50 mg/kg) of protease inhibitor in 70% propylene glycol, 30% ethanol, and 5% dimethyl sulfoxide or by oral gavage with a homogenous dosing solution (1–50 mg/kg) of 4% dimethyl sulfoxide and 96% soybean oil. Similarly, intravenous and oral gavage (via gastric tube) dosings of compounds in identical vehicles were performed on cynomolgous monkeys

Table 1: Enzyme Inhibitory, Antiviral, and Pharmacokinetic Properties of Tripeptide Analogue HIV-1 Protease Inhibitors[a]

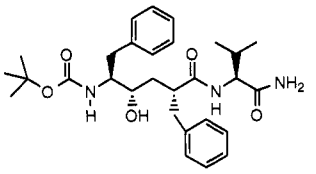

1

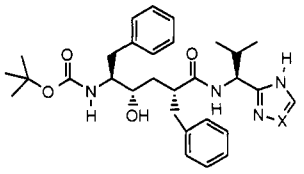

2, X = C-H

3, X = N

compound	K_i (nM)	IC_{50} (μM)	elimination half-life $t_{1/2\beta}$ (min) (rat)	elimination half-life $t_{1/2\beta}$ (min) (monkey)	oral bioavailability F (rat)	oral bioavailability F (monkey)
1	1.4	0.028	13	nd	0.01	nd
2	18	0.57	37	84	0.3	0.14
3	4.2	1.3	23	nd	<0.01	nd

[a] Values were obtained as described in the text. K_i values were determined with recombinant HIV-1 protease. The IC_{50} value is the concentration of inhibitor that inhibits acute viral infectivity in Molt 4 cells by 50%. The measurements of the elimination half-life ($t_{1/2\beta}$) and oral bioavailability (F) of the compounds in rats and monkeys were determined as described in the text. nd, not determined.

(4–5 kg) bearing vascular access ports for sample administration and collection. Dosing and sample collection was performed in conscious rats and monkeys; postdosing blood samples were collected at 0–1440 min, and plasma samples were prepared in 10% sodium citrate. Inhibitors were extracted from the plasma samples in a 4-fold excess of acetonitrile, the extracts were then concentrated to dryness, and the residues were dissolved in dimethyl sulfoxide. Concentrations of inhibitors recovered from the plasma samples were determined by HIV-1 protease inhibition as described (Dreyer et al., 1992), and their plasma concentrations were quantified by use of standard curves of known concentrations of the inhibitors extracted from blood plasma samples prepared in an identical fashion to the unknown samples. Plots of the plasma concentrations vs time for the intravenously and orally administered inhibitors were analyzed for the pharmacokinetic parameters of elimination half-life ($t_{1/2\beta}$) and area-under-curve (AUC) using the in-house computer program #PROTOCOL. Four or more rats and three monkeys were used per study.

RESULTS AND DISCUSSION

Characterization of HIV-1 Protease Inhibitors. Compound **1** (Table 1), a hydroxyethylene-containing tripeptide analogue, constitutes a minimal structure for potent inhibition of the protease (K_i = 1.4 nM) (Dreyer et al., 1992; Abdel-Meguid, 1993). On the basis of the crystal structures of larger HIV-1 protease inhibitors containing hydroxyethylene isosteres within the tripeptide Phe-Phe-Val (Dreyer et al., 1992), it was shown that the six heteroatoms within this tripeptide form hydrogen bonds that are essential for tight binding to the enzyme. The carbonyl oxygen and nitrogen atoms of the C-terminal carboxamide group of **1** are expected to form hydrogen bonds with the Asp29 α-amino group and the Gly48 carbonyl of HIV-1 protease, respectively. Using compound **1** as a template, we designed additional inhibitors in which heterocyclic groups were used as isoelectronic surrogates of the terminal carboxamide group of **1**.

Compound **2** contains an imidazole ring, the N-1 and N-3 atoms of which act as replacements for the amide nitrogen

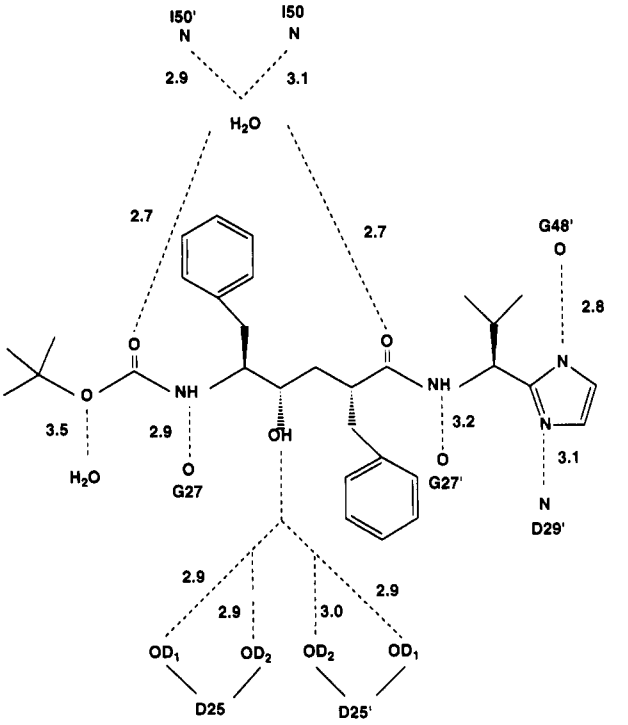

FIGURE 1: Schematic representation of crystallographic data of the HIV-1 protease–compound **2** complex, displaying potential hydrogen-bond interactions between the inhibitor and the enzyme and indicating measured interatomic distances between pairs of hydrogen-bonded atoms.

and carbonyl oxygen of the C-terminal carboxamide in compound **1**. Compound **2** (K_i = 18 nM) is only 10-fold less potent than **1** as an inhibitor of the protease, suggesting that the imidazole may indeed form the same hydrogen bonds with the enzyme as the amide. If the imidazole group of the protease-bound form of **2** were unprotonated, then N-1 and N-3 could be expected to establish hydrogen bonds similar to those observed in other protease–inhibitor complexes. If protonated in the enzyme binding site, the resulting imidazolium ion could form an ionic interaction with the β-carboxyl group of Asp29. At pH 6.0, however, the imidazole group of compound **2** is likely to be predominantly protonated. We have found that the K_i value of **2** increases below pH 6.0, suggesting that the neutral species of **2** is a better inhibitor than the protonated form. This indicates that, at pH 6.0, the inhibitory potency of the less abundant, neutral species of **2** may be similar to that of compound **1** despite the 10-fold difference in apparent K_i.

The triazole analogue (**3**) maintains the hydrogen-bonding capability of **2** and is a more potent inhibitor (Table 1). Since the pK_a of a triazole, in general, is lower than that of an imidazole, the more potent inhibition by **3**, which is presumably unprotonated at pH 6.0, may indicate that the neutral forms of these inhibitors are the true species that bind to the enzyme.

Compound **2** is a considerably less potent inhibitor of the highly related (Grant et al., 1991) retroviral proteases from SIV (K_i = 960 nM) or HIV-2 (K_i = 1280 nM). In addition, inhibition of the monomeric aspartic proteases by compound **2** is very poor: porcine pepsin (K_i = 5000 nM), human renin (K_i = 500 000 nM), and human cathepsin D (K_i = 1200 nM), indicating that the compound is highly selective for inhibition of HIV-1 protease.

Crystallographic Analysis of HIV-1 Protease-Compound 2 Complex. To confirm our design hypothesis and to assist in the design of more potent analogues of compound **2**, we

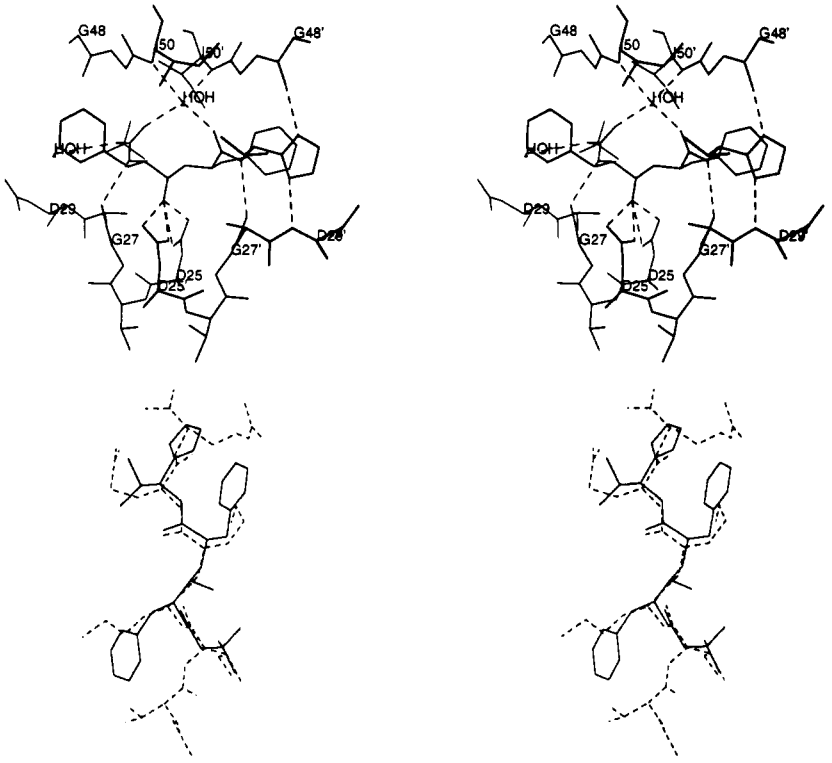

FIGURE 2: (a, top) Stereoview of the crystal structure of compound **2** bound in the active site of HIV-1 protease. Active site amino acid residues forming potential hydrogen bonds with the inhibitor are labeled by one-letter codes. Potential hydrogen bonds are indicated by dotted lines, while circles designate water molecules. (b, bottom) Stereoview of the overlay of the HIV-1 protease-bound conformation of compound **2** (solid lines) and that of MVT-101 (dotted lines; Miller et al., 1989). Overlay was achieved by superposition of the protein backbone atoms of the two complexes.

have determined the crystal structure of the HIV-1 protease–compound **2** complex. The overall three-dimensional structure of the complex is similar to previously reported structures of HIV-1 protease–inhibitor complexes (Fitzgerald, 1993; Wlodawer & Erickson, 1993), where the protease dimer embraces the inhibitor and shields it from bulk solvent. The inhibitor is held in the active site, in an extended conformation, by a set of hydrophobic and hydrogen-bonding interactions. Figure 1 shows the interatomic distances of potential hydrogen bonds between the inhibitor and residues of the active site cleft. Every heteroatom of the inhibitor is hydrogen-bonded to an atom of the protein, either directly or indirectly through a water molecule. The water molecule centrally located on the enzyme's 2-fold axis near the "flaps", found in all HIV-1 protease–inhibitor complexes, is also present in the structure of the HIV-1 protease–compound **2** complex. This water molecule bridges the inhibitor and the protein by forming hydrogen-bonds with the carbonyl oxygens at P_2 and P_1' on one side, and with the amide nitrogens of Ile50 and Ile50′ of the flaps on the other side. Each of the hydrogen bond distances is within the range reported for such a bond in structures of other HIV-1 protease–inhibitor complexes.

N-1 of the imidazole ring is positioned such that it mimics the amide nitrogen of P_3', while N-3 mimics the carbonyl oxygen of P_2' (Figure 2a). Superposition of the bound conformation of compound **2** with that of MVT-101 (Miller et al., 1989), another HIV-1 protease inhibitor (Figure 2b), supports this assertion. Thus, the imidazole ring of compound **2**, clearly, acts as a structural surrogate of the P_2'–P_3' peptide bond, as was hypothesized during the design of the molecule.

The imidazole of compound **2** shows no interactions with the β-carboxylic group of Asp29′, suggesting that the bound imidazole is unprotonated (Figure 2a). Direct determination of proton positions is not possible from X-ray diffraction studies; it would require additional experiments such as neutron diffraction. The apparent absence of interactions between the imidazole and the β-carboxylic group of Asp29′ could also be due to the immobilization of the carboxylic group, through a pair of hydrogen bond interactions with Arg8 and Arg87′. Each of the two carboxylate oxygens forms a hydrogen bond (3.0 Å; mean distance) with one of the terminal side chain nitrogens of each arginine residue. Such interactions have been previously observed in the structures of other HIV-1 protease–inhibitor complexes (Miller et al., 1989). The proximity of the side chains of Asp29′ and Arg8 to the imidazole, however, suggested the design of a number of inhibitors that could establish additional hydrogen bonds with the protein. Of these, the triazole **3** showed enhanced potency and could be forming additional interactions with either or both of these two residues. Unfortunately, we were unsuccessful in cocrystallizing compound **3** with HIV-1 protease.

Antiviral Activity of HIV-1 Protease Inhibitors. We assessed the ability of the heterocycle-containing tripeptide analogue inhibitors to block the acute infectivity of HIV-1 added to virus-naive $CD4^+$ T-lymphocytes (Molt 4 cells). HIV-1 infectivity in cell cultures was quantified at 7 days postinfection as the amount of reverse transcriptase activity present in inhibitor-treated compared to untreated control cultures. As summarized in Table 1, the ability of the inhibitors to block acute infectivity was roughly proportional to their K_i values as has been observed for a large number of compounds of this structural class (Dreyer et al., 1992). Compound **1** is an order of magnitude more potent than **2** in both the enzyme and cell-based assays. However, compound **1** is conspicuously more active in cells than **3** despite their similar K_i values, possibly indicating that the carboxamide-containing inhibitor is better able to enter infected T-lymphocytes than its triazole-bearing analogue.

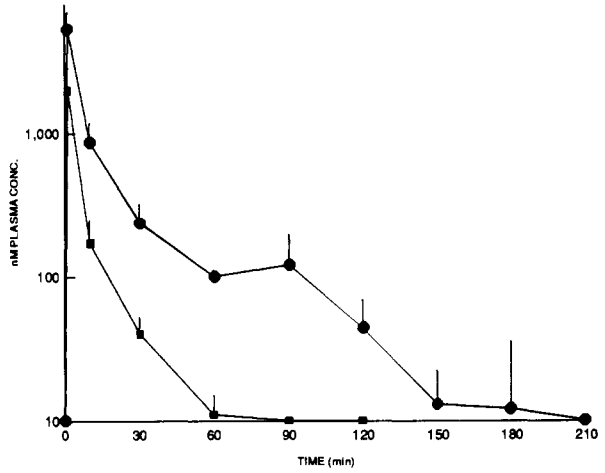

FIGURE 3: Time course of elimination of compounds **1** and **2** from rats following intravenous bolus injection (1 mg/kg dose). The plasma concentrations of the inhibitors following administration were determined by enzyme inhibition assays of plasma extracts as described in the text. Compound **1** (squares); compound **2** (octagons).

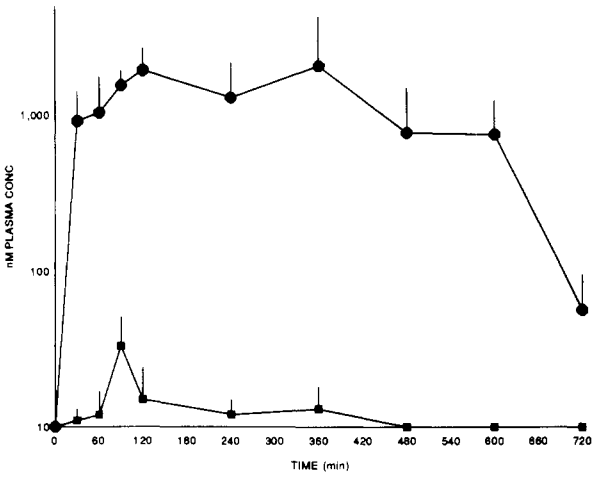

FIGURE 4: Time course of elimination of compounds **1** and **2** from rats following administration by oral gavage (25 mg/kg dose). The plasma concentrations of the inhibitors following administration were determined by enzyme inhibition assays of plasma extracts as described in the text. Compound **1** (squares); compound **2** (octagons).

Pharmacokinetics and Bioavailability of the Heterocycle-Containing HIV-1 Protease Inhibitors. Upon bolus intravenous administration into conscious rats, the tripeptide analogue **1** displayed a very short elimination half-life ($t_{1/2\beta}$ = 13 min; Table 1 and Figure 3), which is typical of highly lipophilic oligopeptide analogues (Greenlee, 1990). Substitution of the terminal carboxamide of **1** with the imidazole of **2** results in a 3-fold increase in the elimination phase half-life of the compound in rat ($t_{1/2\beta}$ = 37 min; Figure 3). The imidazole moiety of **2** is likely to render the tripeptide analogue less lipophilic than **1**, and perhaps makes **2** less susceptible to hepatobiliary extraction (found to be a significant pathway of the excretion of these compounds). Compound **2** was eliminated from rats with a mean systemic plasma clearance rate of 42 mL/min·kg. Compound **2** exhibited a considerably longer elimination phase upon intravenous administration to conscious cynomolgous monkeys ($t_{1/2\beta}$ = 84 min.). The triazole **3** in rats displayed a half-life of elimination substantially less than that of compound **2** ($t_{1/2\beta}$ = 23 min; Table 1).

The substitution of an imidazole moiety for the C-terminal amide group of **1** dramatically improves the oral bioavailability of the compound (Table 1 and Figure 4). In rats, increasing plasma levels of compound **2** were obtained in a dose-dependent manner following administration by oral gavage; the maximum concentration (C_{max}) of **2** varied proportionately from 300–2000 nM at increasing doses of 5–50 mg/kg. The calculated oral bioavailability of compound **2** in rats was 30%. Compound **2** also exhibited significant oral bioavailability in monkeys (14%). In contrast, the oral bioavailability of **1** in the same vehicle in rats was negligible (Figure 4). Thus, the substitution of a carboxamide by the C-terminal imidazole improves the *in vivo* bioavailability properties of the tripeptide analogue in two species. Compound **1** was poorly soluble in the soybean oil vehicle within which **2** was readily dissolved, suggesting that the enhanced solubility conferred by the imidazole group may allow more efficient uptake of the inhibitor into the intestinal mucosa. Interestingly, the triazole **3** displayed good solubility in the vehicle but negligible oral bioavailability in rats, demonstrating that oral absorption of this series of peptide analogues is highly selective and sensitive to small changes in structure.

Compound **2** comprises an important advancement in the development of useful peptidomimetic inhibitors of HIV-1 protease with pharmacokinetic properties that are amenable to drug development. Although it is presently unclear exactly which properties of the imidazole ring result in the enhancement of the pharmacokinetic properties, the benefits of this amide surrogate are probably manifold. While vehicle solubility is clearly improved by this substitution, it is likely that the substitution also favorably influences both metabolic stability and clearance and perhaps results in enhanced penetration of the intestinal mucosa.

ACKNOWLEDGMENT

We thank Drs. C. Debouck, M. Rosenberg, J. Gleason, J. Baldoni, and P. Dalmonte for their contributions to this research. We also to thank L. Gutshall, T. Lewandowski, D. Maley, J. Morris, E. Sternberg, and G. Wells for their technical assistance.

REFERENCES

Abdel-Meguid, S. S. (1993) *Med. Res. Rev. 13*, 731–778.

Abdel-Meguid, S. S., Zhao, B., Murthy, K. H. M., Winborne, E., Choi, J.-K., DesJarlais, R. L., Minnich, M. D., Culp, J. S., Debouck, C., Tomaszek, T. A., Jr., Meek, T. D., & Dreyer, G. B. (1993) *Biochemistry 32*, 7972–7980.

Bernstein, F. C., Koetzle, T. F., Williams, G. J., Meyer, E. E. J., Brice, M. D., Rodgers, J. R., Kennard, O., Shimanouchi, T., & Tasumi, M. (1977) *J. Mol. Biol. 112*, 535–542.

Brunger, A. T., Kuriyan, J., & Karplus, M. (1987) *Science 235*, 458–460.

Debouck, C., Gorniak, J. G., Strickler, J. E., Meek, T. D., Metcalf, B. W., & Rosenberg, M. (1987) *Proc. Natl. Acad. Sci. U.S.A. 84*, 8903–8906.

Dreyer, G. B., Lambert, D. M., Meek, T. D., Carr, T. J., Tomaszek, T. A., Jr., Fernandez, A. V., Bartus, H., Cacciavillani, E., Hassell, A., Minnich, M., Petteway, S. R., Jr., Metcalf, B. W., & Lewis, M. (1992) *Biochemistry 31*, 6646–6659.

Dreyer, G. B., Boehm, J. C., Chenera, B., DesJarlais, R. L., Hassell, A. M., Meek, T. D., Tomaszek, T. A., Jr., & Lewis, M. (1993) *Biochemistry 32*, 937–947.

Erickson, J., Neidhart, D. J., VanDrie, J., Kempf, D. J., Wang, X. C., Norbeck, D. W., Plattner, J. J., Rittenhouse, J. W., Turon, M., Wideburg, N., Kohlbrenner, W. E., Simmer, R., Helfrich, R., Paul, D. A., & Knigge, M. (1990) *Science 249*, 527–533.

Fitzgerald, P. M. D. (1993) *Curr. Opin. Struct. Biol. 3*, 868–874.

Goel, O. P., Krolls, U., Stier, M., & Kesten, S. (1989) *Org. Synth. 67*, 69–75.

Grant, S. K., Deckman, I. C., Minnich, M. D., Culp, J., Franklin, S., Dreyer, G. B., Tomaszek, T. A., Jr., Debouck, C., & Meek, T. D. (1991) *Biochemistry 30,* 8424–8434.

Greenlee. W. J. (1990) *Med. Res. Rev. 10,* 173–236.

Hendrickson, W. A. (1985) *Methods Enzymol. 115,* 252–270.

Howard, A. J., Gilliland, G. L., Finzel, B. C., Poulos, T. L., Ohlemdorf, D. H., & Salemme, F. R. (1987) *J. Appl. Crystallogr. 20,* 383–387.

Jones, T. A. (1985) *Methods Enzymol. 115,* 157–171.

Lambert, D. M., Petteway, Jr., S. R., Jr., McDanal, C. E., Hart, T. K., Leary, J. J., Dreyer, G. B., Meek, T. D., Bugelski, P. J., Bolognesi, D. P., Metcalf, B. W., & Matthews, T. J. (1992) *Antimicrob. Agents Chemother. 36,* 982–988.

McPherson, A. J. (1976) *Methods Biochem. Anal. 23,* 249–345.

Meek, T. D. (1992) *J. Enzyme Inhib. 6,* 65–98.

Meek, T. D., Dayton, B. D., Metcalf, B. W., Dreyer, G. B., Strickler, J. E., Gorniak, J. G., Rosenberg, M., Moore, M. L., Magaard, V. W., & Debouck, C. (1989) *Proc. Natl. Acad. Sci. U.S.A. 86,* 1841–1845 (1989).

Meek, T. D., Lambert, D. M., Metcalf, B. W., Petteway, S. R., Jr., & Dreyer, G. B. (1990a) in *Design of Anti-AIDS Drugs* (DeClercq, E., Ed.) pp 225–256, Elsevier, Amsterdam.

Meek, T. D., Lambert, D. M., Dreyer, G. B., Carr, T. J., Tomaszek, T. A., Jr., Moore, M. L., Strickler, J. E., Debouck, C., Hyland, L. J., Matthews, T. J., Metcalf, B. W., & Petteway, S. R. (1990b) *Nature 343,* 90–92.

Miller, M., Schneider, J., Sathyanarayana, B. K., Toth, M. V., Marshall, G. R., Clawson, L., Selk, L., Kent, S. B. H., & Wlodawer, A. (1989) *Science 246,* 1149–1152.

Ratner, L., Haseltine, W., Pataraca, R., Livak, K. J., Starcich, B., Josephs, S. F., Doran, E. R., Rafalski, J. A., Whitehorn, E. A., Baumeister, K., Ivanoff, L., Petteway, S. R., Jr., Pearson, M. L., Lautenberger, L. A., Papas, T. S., Ghrayeb, J., Chang, N. T., Gallo, R. C., & Wong-Staal, F. (1985) *Nature 313,* 277–284.

Smith, J. L., Corfield, P. W., Hendrickson, W. A., & Low, B. W. (1988) *Acta Crystallogr. A44,* 357–368.

Wlodawer, A., & Erickson, J. W. (1993) *Annu. Rev. Biochem. 62,* 5434–5485.

Wlodawer, A., Miller, M., Jaskolski, M., Sathyanarayana, B. K., Baldwin, E., Weber, I. T., Selk, L. M., Clawson, L. Schneider, J., & Kent, S. B. H. (1989) *Science 245,* 616–621.